

# Improving a commercially available heterodyne laser interferometer to sub-nm uncertainty

H. Haitjema, S.J.A.G. Cosijns, N.J.J. Roset and M.J.Jansen

Eindhoven University of Technology, PO Box 513, 5600 MB Eindhoven, The Netherlands

## ABSTRACT

Laser interferometer systems are known for their high resolution, and especially for their high range/resolution ratio. In dimensional metrology laboratories, laser interferometers are popular workhorses for the calibration of displacements. The uncertainty is usually limited to about 10 nm due to polarization- and frequency mixing. For demanding applications however nanometer uncertainty is desired. We adapted a commercially available heterodyne laser interferometer by feeding the measurement signal into a fast lock-in amplifier and use the laser interferometer reference signal as a reference. By measuring both the in-phase and quadrature component an uncorrected phase can be directly measured. By recording both components while the phase changes between 0 and  $2\pi$  a typical ellipse is recorded from which the first and second harmonics of periodic deviations can be derived. These can be corrected independent of their origin. Measurements using a Babinet-Soleil compensator show that this method can reduce significant non-linearities (16 nm top-bottom) to a standard deviation down to about 0.01 nm. This is confirmed in the evaluation of some standard optical-set-ups. With this method, also optical set-ups can be analysed to predict the non-linearities when a non-compensated standard interferometer is used.

**Keywords:** Laser interferometry, heterodyne, sub-nm, non-linearity, correction

## 1. INTRODUCTION

Laser interferometer systems are known for their high resolution, and especially for their high range/resolution ratio. In dimensional metrology laboratories, laser interferometers are popular workhorses for the calibration of displacements. Their uncertainty is limited to the refractive index of air for long range. For short range calibration the limitations are in the photonic noise and residual nonlinearities repeating each fraction of a wavelength. The nonlinearities can be present in the phase measurement system of the interferometer itself,<sup>1</sup> but they can also result from polarization states of the laser and the optics used: beam splitters, retardation plates used with plane mirrors and corner cubes can influence the polarization state in interferometers using polarizing optics, or influence the contrast in interferometers with non-polarizing optics. Compensation of nonlinearities becomes important within the nanometer region. For homodyne laser interferometers the compensation method of Heydemann<sup>2</sup> is used widely.<sup>3</sup> A quadrature phase measurement method in combination with a lock-in amplifier was used previously to compensate a heterodyne interferometer with a split frequency of 160 kHz.<sup>4</sup> We are using a combination of both methods for a commercial heterodyne laser interferometer with a split frequency of 2.7 MHz and compare the results with calculations using a theoretical model.

## 2. PRINCIPLE OF HETERODYNE LASER INTERFEROMETRY

The laser shown in figure 1 consists of a laser source which emits two orthogonal polarized beams with a different frequency ( $f_1$  and  $f_2$ ). These two beams can be represented as:

$$E_1 = E_0 \sin(2\pi f_1 t + \phi_{01}) \quad (1)$$

$$E_2 = E_0 \sin(2\pi f_2 t + \phi_{02}). \quad (2)$$

---

Further author information: (Send correspondence to H.Haitjema)

S.J.A.G.Cosijns: E-mail: s.j.a.g.cosijns@tue.nl, Phone: +31 (0)40 247 2620

H.Haitjema: E-mail: h.haitjema@tue.nl

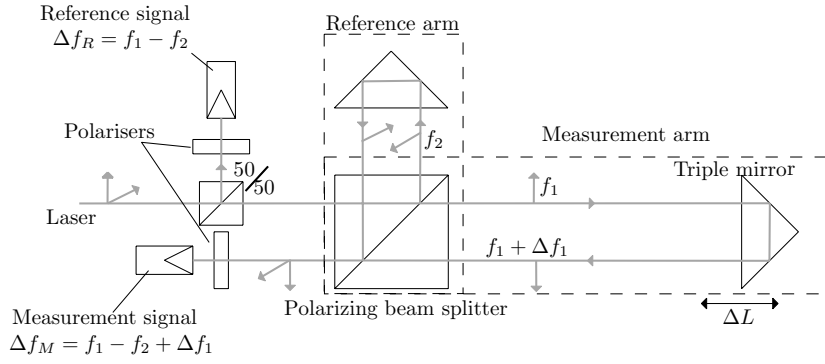


**Figure 1.** Schematical representation of the principle of a heterodyne laser interferometer.

A non-polarizing beam splitter divides the beam in two parts: one reference part and one measurement part. The reference part passes a combining polarizer and a detector resulting in an interference signal of which only the alternating current is measured using a band-pass filter, eliminating both the DC component and optical frequencies. This signal can be represented by:

$$I_{ref} = \frac{1}{2} E_0^2 [\cos(2\pi(f_1 - f_2)t + (\phi_{01} - \phi_{02}))]. \quad (3)$$

The measurement part is divided by a polarizing beam splitter in a reference arm and in a measurement arm. The signal in the measurement arm receives a Doppler shift as a result of the moving corner cube, resulting in a phase shift of the measurement signal compared to the reference signal<sup>5</sup>:

$$\Delta\phi_1 = 2\pi\Delta f_1 t = \frac{4\pi n\Delta l}{\lambda_1}. \quad (4)$$

with  $\lambda_1$  representing the wavelength of the light reflected by the mirror and  $n$  the refractive index of air in the measurement path. With a polarizer the signal from the reference arm and the signal from the measurement arm are combined and result in an interference pattern. From this interference pattern the measurement signal is constructed containing the phase information and therefore containing the displacement of the corner cube. In an ideal laser interferometer  $E_1$  enters the measurement arm and  $E_2$  enters the reference arm and the detected signal can be represented by:

$$I_{meas} = \frac{1}{2} E_0^2 [\cos(2\pi(f_1 - f_2)t + (\phi_{01} - \phi_{02}) + \Delta\phi_1)]. \quad (5)$$

Where  $f_1$  and  $f_2$  are the frequency of measurement and reference arm,  $\phi_{01}$  and  $\phi_{02}$  are the initial phase of both frequencies and  $\Delta\phi_1$  is the phase difference as a result of the target movement. The measurement with a laser interferometer is based on measuring the phase difference between the measurement signal (5) and the reference signal (3). In a common laser interferometer the separation between both arms and therefore both polarization states is not ideal, part of the measurement frequency enters the reference arm and part of the reference frequency enters the measurement arm and gets a Doppler shift also. This results in an extra phase term in the measurement signal which now can be represented as:

$$I_{measnl} = \frac{1}{2} E_0^2 [\cos(2\pi(f_1 - f_2)t + (\phi_{01} - \phi_{02}) + \Delta\phi_1 + \Delta\phi_{nonlin})]. \quad (6)$$

The calculation in the interferometer however uses only one frequency resulting in non-linearities in the measurement results. The extra phase term therefore represents the non-linearity of the system.

### 3. PRINCIPLE OF QUADRATURE DETECTION WITH A LOCK-IN AMPLIFIER

A lock-in amplifier enables the phase detection between two signals with the same carrier frequency, due to a method called Phase Sensitive Detection. This method enables the filtering of a certain frequency. Noise signals with a different frequency are filtered out. For this method a reference frequency and phase is needed. In the heterodyne laser interferometer 2 signals are generated:

$$I_{ref} = A \sin(2\pi(f_1 - f_2)t + \phi_{ref}) \quad (7)$$

$$I_{meas} = B \sin(2\pi(f_1 - f_2)t + \phi_{meas} + \phi_{nonlin}). \quad (8)$$

Where  $I_{ref}$  is the reference signal and  $I_{meas}$  stands for the measurement signal. These signals can well be analysed using a lock-in amplifier. With use of a mixer these signals are multiplied and passed through a band pass filter:

$$S_0 = \frac{1}{2}AB \cos(\phi_{ref} - \phi_{meas} - \phi_{nonlin}). \quad (9)$$

To enable a phase measurement a second reference signal, retarded  $\frac{\pi}{2}$  in phase, is multiplied with the measurement signal resulting in a sine function:

$$S_{90} = \frac{1}{2}AB \sin(\phi_{ref} - \phi_{meas} - \phi_{nonlin}). \quad (10)$$

From simulations it is known that many harmonics of nonlinearity exist, however the first and second order are dominant.<sup>6</sup> Therefore the above mentioned signals can be rewritten as follows:

$$S_0 = x_0 + R \cos(\phi) \quad (11)$$

$$S_{90} = y_0 + R\left(\frac{1}{r}\right) \sin(\phi - \alpha). \quad (12)$$

Where the offset  $x_0$  and  $y_0$  gives a first order non-linearity and the ellipticity characterized by  $r$  and  $\alpha$  gives the second order non-linearity,  $R$  represents the amplitude of the signals.

### 4. MEASUREMENT RESULTS

With use of a Stanford Research SRS844 lock-in amplifier the phase quadrature measurement is carried out. Both output signals are captured with a PC. After an initiating measurement the ellipse parameters are calculated using a least square fit on the parameters of (11) and (12) using the method by Heydemann.<sup>2</sup> These parameters are used to compensate the interferometer system. The schematical setup is shown in figure 2. Note that Picotto<sup>7</sup> and Sacconi<sup>8</sup> used a similar setup, just he uses a phase detector instead of a lock-in amplifier.

In order to verify the compensation method three kinds of measurements were done. First a measurement of the nonlinearity resulting from a common path setup with use of a Babinet Soleil Compensator replacing the interferometer optics is carried out. The second is a measurement of the entire laser interferometer including the interferometer optics, both linear optics as well as high stable flat mirror optics. The final measurement was a comparison of flat mirror laser interferometer and an inductive probe.

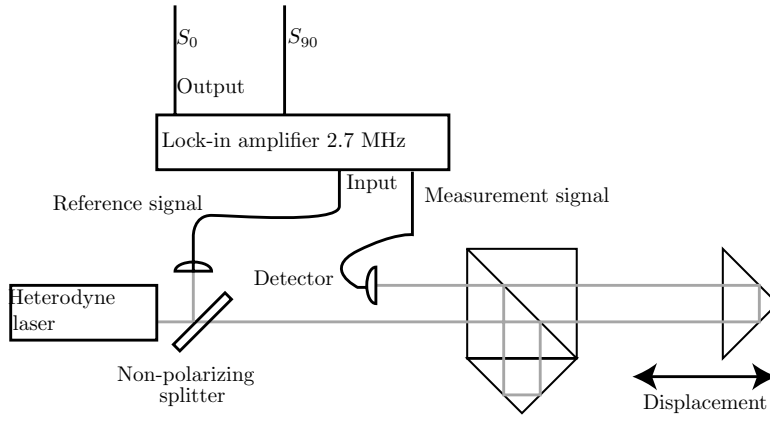


**Figure 2.** Schematical representation of the setup.

#### 4.1. Common path verification

The Babinet Soleil Compensator provides a common path for both polarization components, and therefore cancels out any influence of the refractive index of air. It also provides a convenient way to apply an optical path difference of parts of a wavelength. This optical path difference is produced due to a difference in refractive index for two orthogonal polarization states. The phase difference introduced between both polarization axes can be represented as<sup>9</sup>:

$$\Delta\phi = 2\pi \left| \frac{n_{\perp}}{\lambda_{\perp 0}} - \frac{n_{\parallel}}{\lambda_{\parallel 0}} \right| d. \quad (13)$$

Where  $\lambda_{\perp 0}$  and  $\lambda_{\parallel 0}$  are the vacuum wavelengths of both polarization states,  $n_{\perp}$  and  $n_{\parallel}$  are the refractive indices for both polarization arms and  $d$  represents the thickness of the Babinet Soleil Compensator. By varying the thickness of the compensator (through movement of the wedges compared to each other, see figure 3) the optical path difference between both polarization states can be varied. A rotation of the optics (left in figure 3) around the laser beam axis can be simulated by rotating the Babinet Soleil compensator about the laser beam axis.

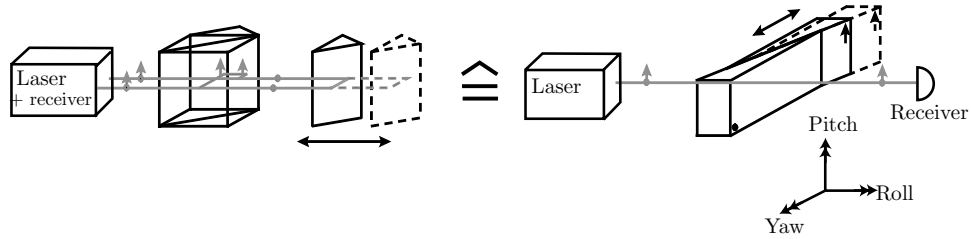


**Figure 3.** Schematical representation of the simulation of the interferometer optics with a Babinet Soleil Compensator.

Measurements were carried out as following: in the experimental setup the Babinet Soleil Compensator is shifted in small steps over a bit more than two wavelength path-difference. Both signals  $S_0$  and  $S_{90}$  are recorded and a least-squares fit to equations 11 and 12 is made. From these data the corrected phase ( $\phi$ ) is derived and compared to the uncorrected phase  $\phi = \arctan^{-1}(\frac{S_{90}}{S_0})$  as it is measured in commercially available systems. A measurement was taken with a rotation of  $10^\circ$  of the Babinet Soleil Compensator. Figure 4 gives the corrected and uncorrected results where on the right the  $S_{90}$  signal is plotted against the  $S_0$  signal and on the left the

phase deviation is re-calculated to a length deviation when linear optics would be used. The deviations from the fitted curve indicate the remaining deviations of the system after correction. Assuming that noise in the recorded intensities can be phase noise as well as amplitude noise, deviations in amplitude can be considered as a possible phase error<sup>10</sup>:

$$\Delta\phi = \frac{\Delta R}{R} \quad (14)$$

Note that this is a worst-case estimation: if the laser intensity fluctuates this will also give an amplitude variation but not a phase variation. The non-linearity as it is measured in figure 4 without correction can be characterised by a standard deviation of 4.4 nm; after correction this is reduced to a standard deviation of 0.008 nm. From model calculations<sup>6</sup> and measurements of the laser polarization state<sup>11</sup> this type of deviation is known; it is also known that the deviation turns into a second-order deviation once the receiver is given the same rotation as the optics (in this case the Babinet Soleil Compensator). The results of this experiment are given in figure 5. Comparing the right hand figures 4 and 5 one can observe that in figure 4 the measured circle is shifted downward relative to the undisturbed corrected circle and becomes somewhat elliptical. In figure 5 the centre point is shifted back and only the ellipticity remains. This is reflected in the fitted parameters:  $r$  and  $\alpha$  are similar in both figures, but in figure 5 the bias in y-direction is almost vanished. This is reflected in a smaller linearity deviation for the uncorrected case at the left-hand of figure 5. In this case the standard deviation of the measurement reduces from 1.17 nm for the uncompensated measurement to below 0.001 nm for the corrected measurement.

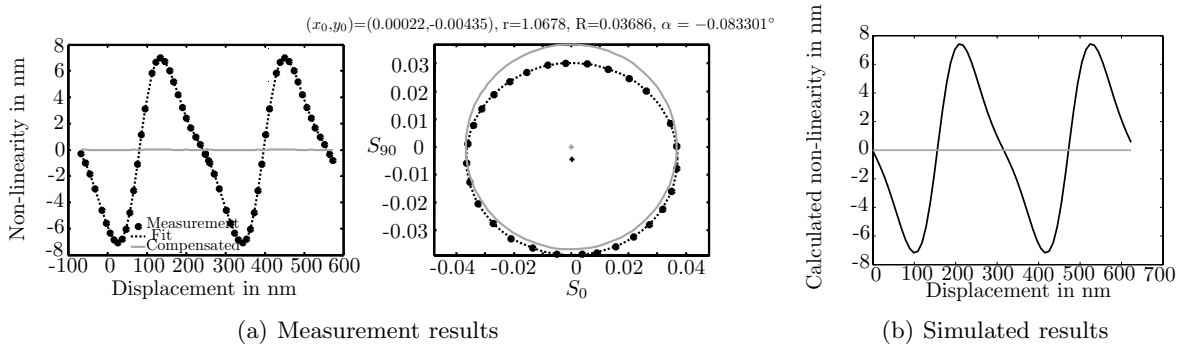


**Figure 4.** Results of a measurement with a rotated Babinet Soleil Compensator 10°.

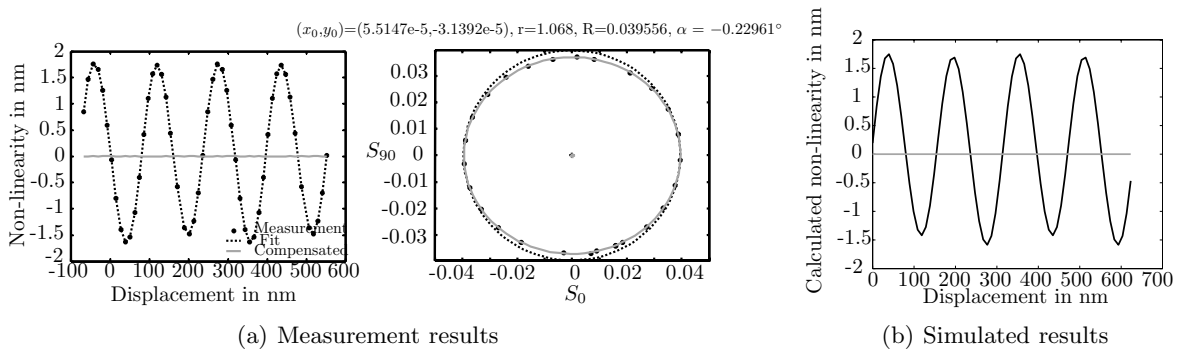


**Figure 5.** Results of a measurement with a rotated Babinet Soleil Compensator and a rotated receiver polarizer (both 10°).

## 4.2. Verification of basic interferometer set-ups

To verify the effect of the optics as predicted in<sup>12</sup> also two setups were built with interferometer optics. One with linear optics and a second one with flat mirror optics. To generate a stable but slowly varying displacement an aluminium distance tube was placed between the polarizing beamsplitter and the measurement optics. The displacement was generated by warming up the tube by hand and then letting it cool down slowly to room temperature. The result for the linear optics is given in figure 6. This figure shows that already without compensation the non-linearity is within 1 nm. The compensation reduces the standard deviation of the non-linearity to 0.0012 nm.

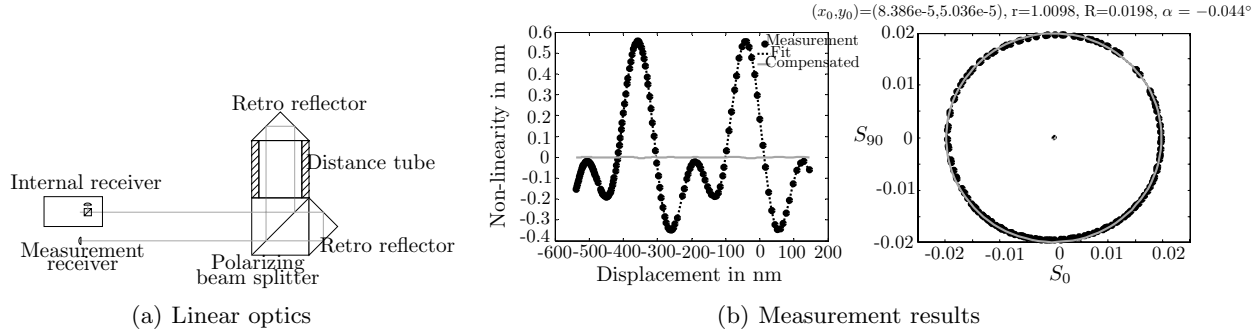


**Figure 6.** Results of a measurement with linear optics.

The flat mirror optics gives a more peculiar behaviour, as depicted in figure 7. The same kind of behaviour was noticed by Číp.<sup>13</sup> By modelling the optics and laser head polarization errors it was tried to explain the deviation. This can be done if the assumption is made that the optics were misaligned by  $4.9^\circ$ . The right hand side of figure 7 gives the result of the model calculation. The model was based on a Jones matrix calculation. The polarization errors of the optics were measured by ellipsometry<sup>12</sup> and the polarization error of the laserhead was measured as explained in.<sup>11</sup> The ellipticity of the laserhead was 1 : 148 for  $f_1$  and 1 : 168 for  $f_2$  in E-field one left hand elliptical and one right hand elliptical. The non-orthogonality between both laser polarizations was  $0.1^\circ$ . The compensation reduces the standard deviation of the non-linearity from 0.35 nm down to 0.002 nm.

## 4.3. Comparison probe and flat mirror optics

In the laboratory of Precision Engineering at Eindhoven University of Technology a calibration system for probes of Coordinate Measuring Machines was developed based on a flat mirror interferometer (see figure 8).

In earlier probe calibrations it appeared to show non-linearities.<sup>14</sup> Therefore this system was tested also. The results are given in figure 9. On the left hand side both uncompensated and compensated data are shown of the setup as shown in figure 8. Due to the probe properties the improvement remains limited. On the right hand of figure 9 the results are shown when the ellipticity of the laser head is increased by means of a rotated  $\frac{\lambda}{4}$ -plate. In this figure the reduction of the second order non-linearity is clearly visible. However a first order non-linearity with the same order of magnitude as for the left-hand of the figure remains. For the future we plan to test the setup on a traceable calibration setup in which no non-linearities are inherent.<sup>15</sup>

## 5. CONCLUSIONS

Phase measurement by lock-in technique was successfully applied to a commercially available heterodyne laser interferometer system operating at a frequency difference of 2.7 MHz. Applying the Heydemann correction to

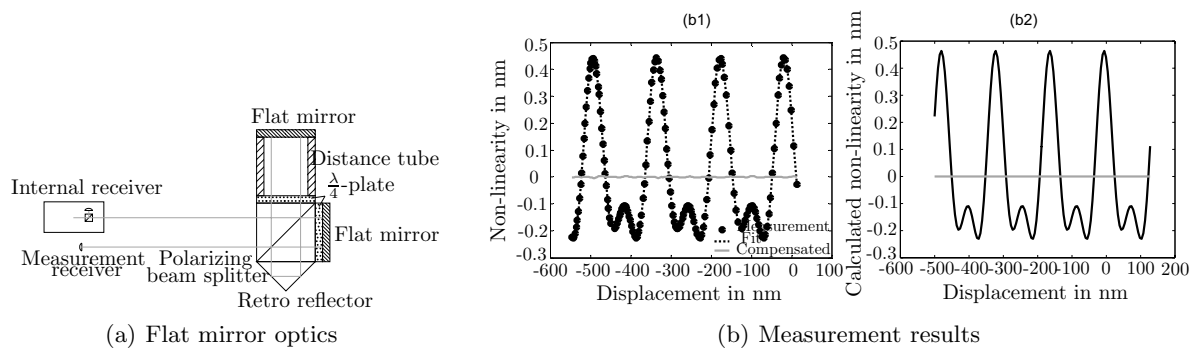


**Figure 7.** Results of a measurement with flat mirror optics (b1) and results of the simulated non-linearity from these optics (b2).

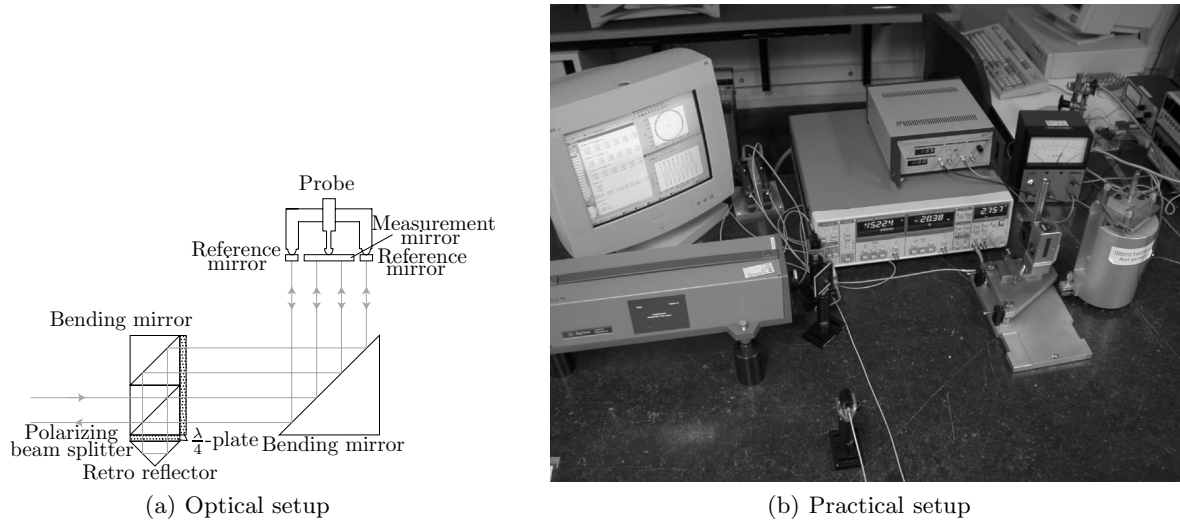


**Figure 8.** Measurement setup.

the measured signals reduces the periodic errors from several nanometers to less than 0.01 nm. The shape of periodic errors found was consistent with model calculations for the used setups. This method can also be used for measuring periodic errors of existing non-compensating setups.

### Acknowledgement

This work was financially supported by the Dutch ministry of economic affairs in the framework of the program "IOP Precisie Technologie".

### REFERENCES

1. P. H. N.M. Oldham, J.A. Kramar and E. Teague, "Electronic limitations in phase meter for heterodyne interferometry," *Precision Engineering* **15**, pp. 173–179, July 1993.
2. P. L. Heydemann, "Determination and correction of quadrature fringe measurement errors in interferometers," *Applied optics* **20**, pp. 3382–3384, October 1981.
3. M.J.Downs and W. Rowley, "A proposed design for a polarisation insensitive optical interferometer system with sub-nanometric capability," *Precision Engineering* **15**, pp. 281–286, October 1993.

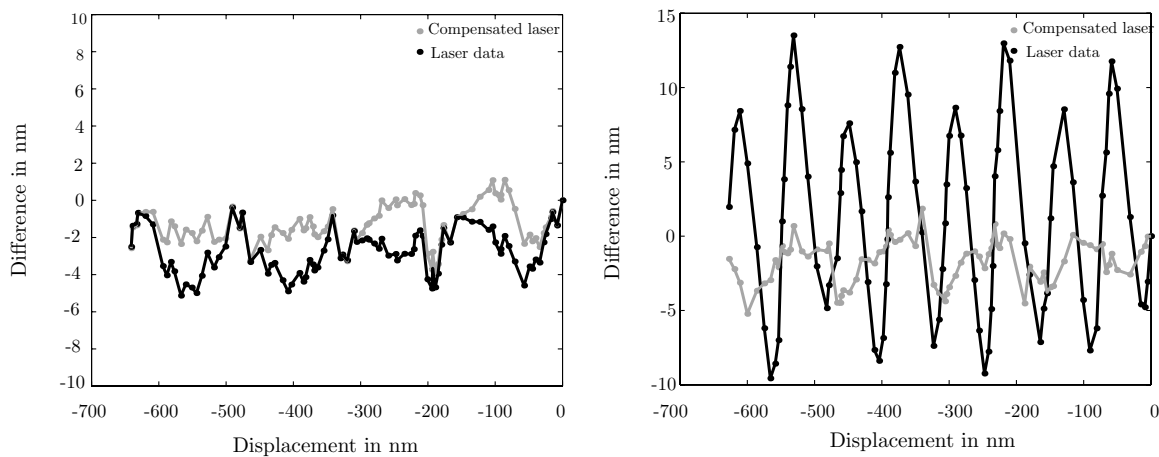


**Figure 9.** Difference between laser and probe.

4. T. C. TaeBong Eom *et al.*, "A simple method for the compensation of the nonlinearity in the heterodyne interferometer," *Measurement Science and Technology* **13**, pp. 222–225, January 2002.
5. Jens Flügge, *Vergleichende untersuchungen zur messtechnischen leistungsfhigkeit von laserinterferometern und inkrementellen masstabmesssystemen*. PhD thesis, Physikalisch Technische Bundesanstalt, February 1996.
6. S. Cosijns, H. Haitjema, and P. Schellekens, "Modelling and verifying non-linearities in heterodyne displacement interferometry," *Precision Engineering* **26**, pp. 448–455, 2002.
7. M. G.B.Picotto, "A sample scanning system with nanometric accuracy for quantitative spm measurements," *Ultramicroscopy* **86**, pp. 247–254, 2001.
8. G. P. A. Sacconi and W. Pasin, "Interferometric calibration of piezo-capacitive displacement actuators," *Proceedings of 4th IMEKO symposium on Laser metrology*, 1996.
9. R. Azzam and N. Bashara, *Ellipsometry and polarized light*, Elsevier Science, Amsterdam, 1999.
10. J. L. Chien-ming Wu and R. D. Deslattes, "Heterodyne interferometer with subatomic periodic nonlinearity," *Applied optics* **38**, pp. 4089–4094, July 1999.
11. D.Lorier, B.Knarren, S.Cosijns, H.Haitjema, and P.Schellekens, "Polarisation state analysis of heterodyne laser beams," *CIRP Annals* **25**, August 2003.
12. S. Cosijns, H. Haitjema, and P. Schellekens, "The influence of polarization states on non-linearities in laser interferometry," *Proceedings of the 3<sup>rd</sup> Euspen International Conference, Eindhoven, The Netherlands*, pp. 593–596, May 2002.
13. O. Cip and F. Petru, "A scale-linearization method for precise laser interferometry," *Meas. Sci. Technol.* **11**, pp. 133–141, 2000.
14. W. Pril, *Development of high precision mechanical probes for coordinate measuring machines*. PhD thesis, TUE, December 2002.
15. H. Haitjema, P. Schellekens, and S. Wetzels, "Calibration of displacement sensors up to 300  $\mu\text{m}$  with nanometre accuracy and direct traceability to a primary standard of length," *Metrologia* **37**(1), pp. 25–33, 2000.